Supporting Information for

Electrospun Micropatterned Nanocomposites Incorporated with Cu_2S Nanoflowers for Skin Tumor Therapy and Wound Healing

*Xiaocheng Wang[1, 2], Fang lv[3], Tian Li[1, 2], Yiming Han[3], Zhengfang Yi[3], Mingyao Liu[3], Jiang Chang[1], Chengtie Wu[1]**

Ms. X. C. Wang, Mr. T. Li, Prof. J. Chang, Prof. C. T. Wu

1. State Key Laboratory of High Performance Ceramics and Superfine Microstructure, Shanghai Institute of Ceramics, Chinese Academy of Sciences, 1295 Dingxi Road, Shanghai 200050, People's Republic of China.

Ms. X. C. Wang, Mr. T. Li

2. University of Chinese Academy of Sciences, 19 Yuquan Road, Beijing 100049, People's Republic of China.

Ms. F. Lv, Ms. Y. M. Han, Prof. M.Y. Liu, Prof. Z. F. Yi

3. Shanghai Key Laboratory of Regulatory Biology, Institute of Biomedical Sciences and School of Life Sciences, East China Normal University, 500 Dongchuan Road, Shanghai 200241, People's Republic of China.

*** Corresponding author:**

Chengtie Wu

E-mail: chengtiewu@mail.sic.ac.cn (C. Wu); Tel: +86-21-52412249.

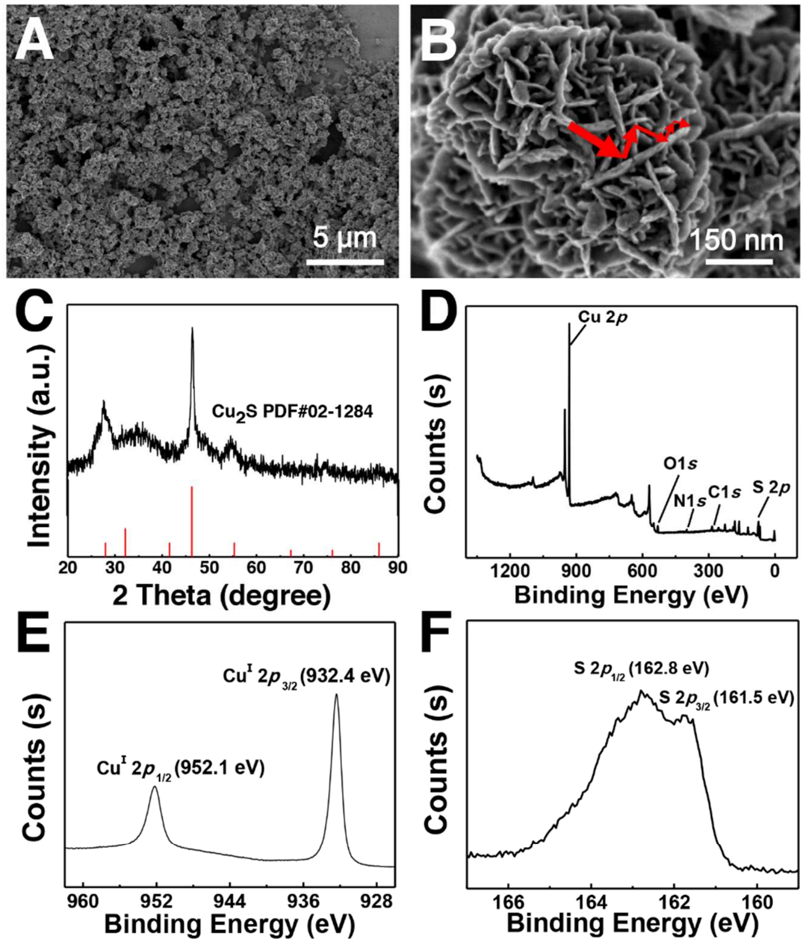

Figure S1. Characterization of Cu_2S particles. (A, B) SEM images, (C) XRD pattern and (D) XPS spectrum of Cu_2S particles. XPS characteristic spectrum for (E) Cu 3p and (F) S 2p electrons of Cu_2S particles, indicating valence state of +1 and -2 for Cu and S, respectively.

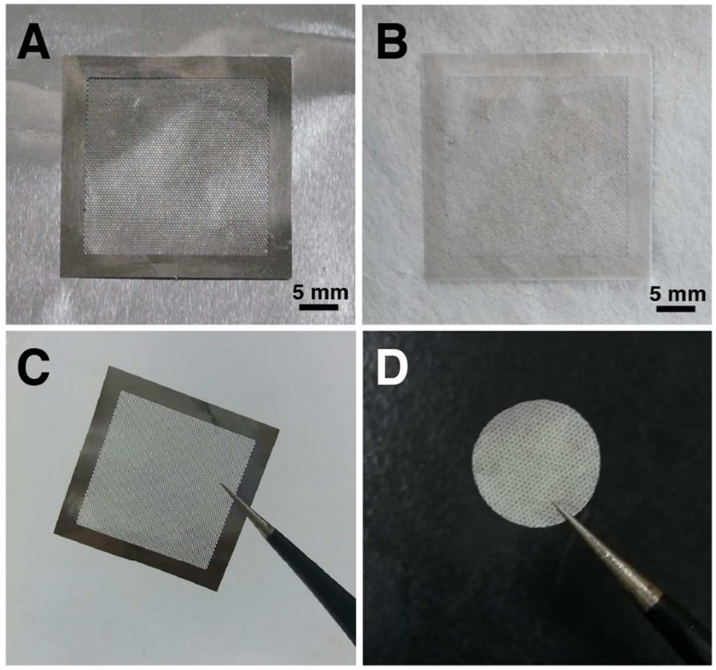

Figure S2. Photograph of (A) a custom-made stainless steel mesh (pore diameter: 300 μm) horizontally fixed on the conductive plate as the fiber collector, (B) electrospun fibers directly deposited on the surface of the mesh, (C) a steel mesh and (D) CS-PLA/PCL membranes (diameter: 10 mm) held by tweezers.

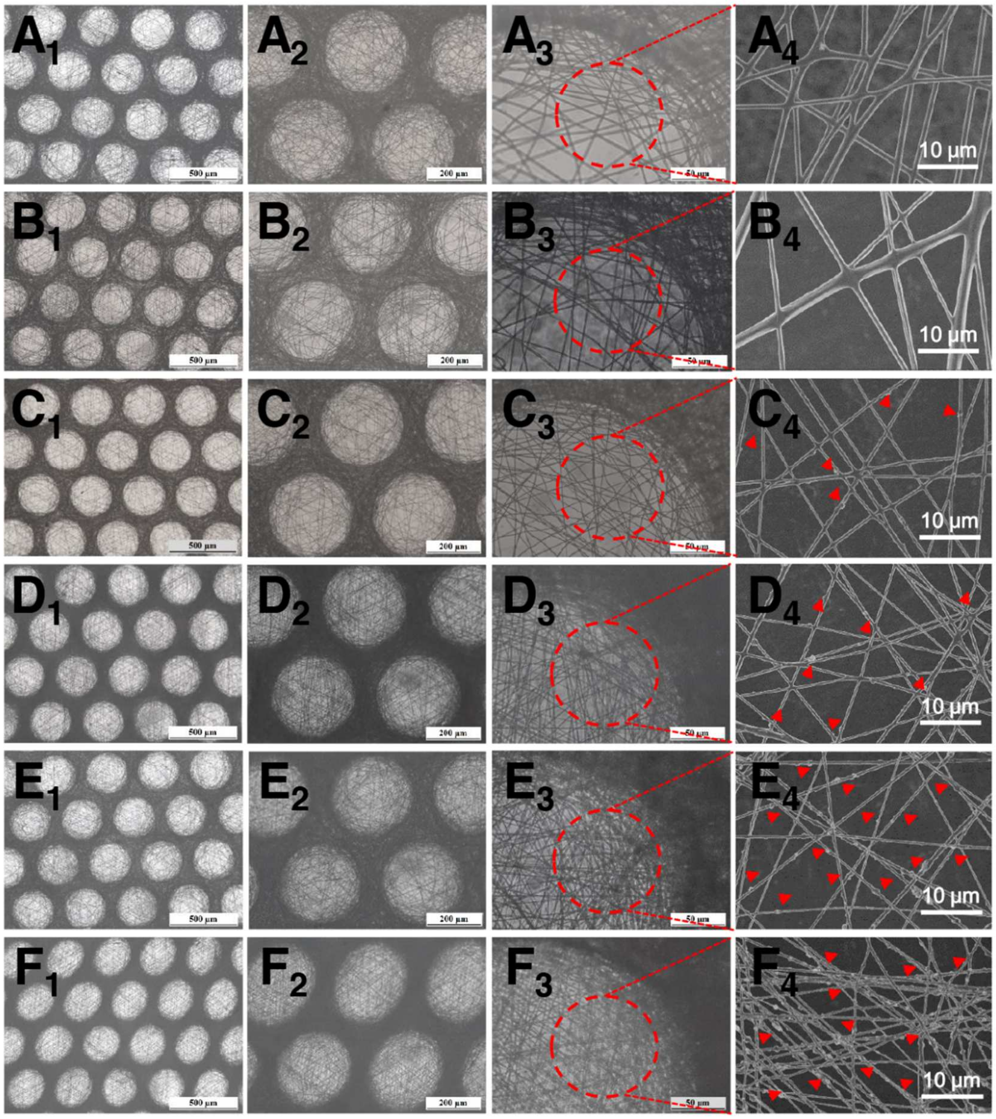

Figure S3. Morphologies of CS-PLA/PCL membranes. Representative optical images of (A_{1-3}) 0CS-PLA/PCL, (B_{1-3}) 10CS-PLA/PCL, (C_{1-3}) 20CS-PLA/PCL, (D_{1-3}) 30CS-PLA/PCL, (E_{1-3}) 40CS-PLA/PCL, (F_{1-3}) 50CS-PLA/PCL membranes at different magnification and corresponding (A_4-F_4) SEM images of fibers in the micropatterned macropores of CS-PLA/PCL membranes, indicating the successful integration with Cu_2S nanopaticles (shown by red arrows) into the polymer fibers.

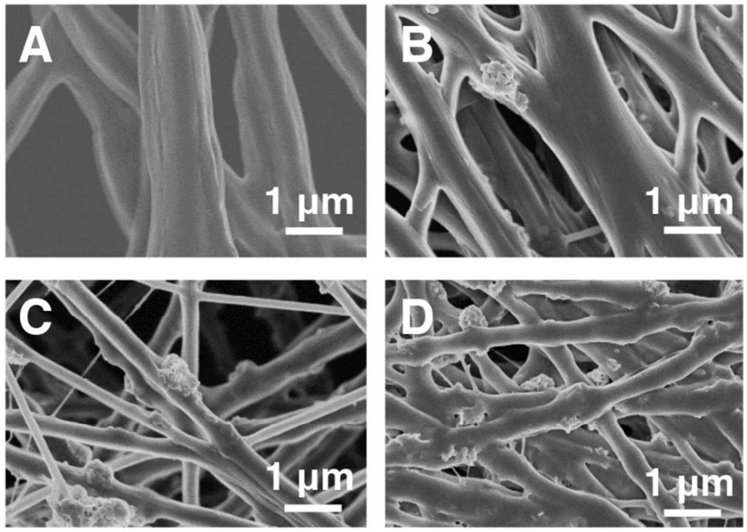

Figure S4. Representative high-resolution SEM images of (A) 10CS-, (B) 20CS-, (C) 40CS-and (D) 50CS-PLA/PCL membranes. With the increase of Cu_2S content in the precursor dispersion, the particle amount in the fibers proportionally increased.

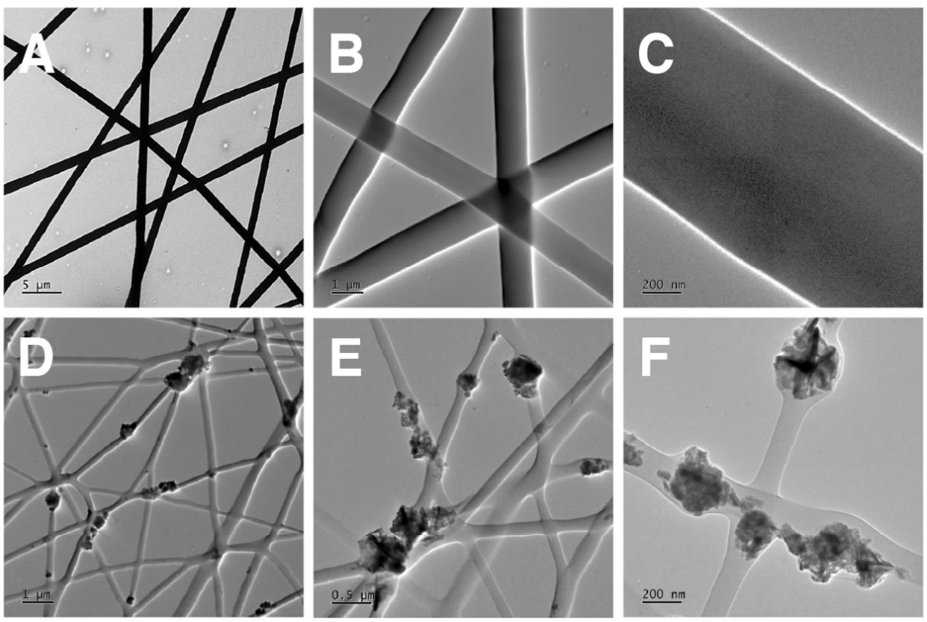

Figure S5. Representative TEM images of (A-C) 0CS- and (D-F) 30CS-PLA/PCL membranes at different magnification. The particles could not be fully embedded into the Cu_2S-incorpated electrospun fibers, which led to the fibers with rougher surface than unloaded membranes.

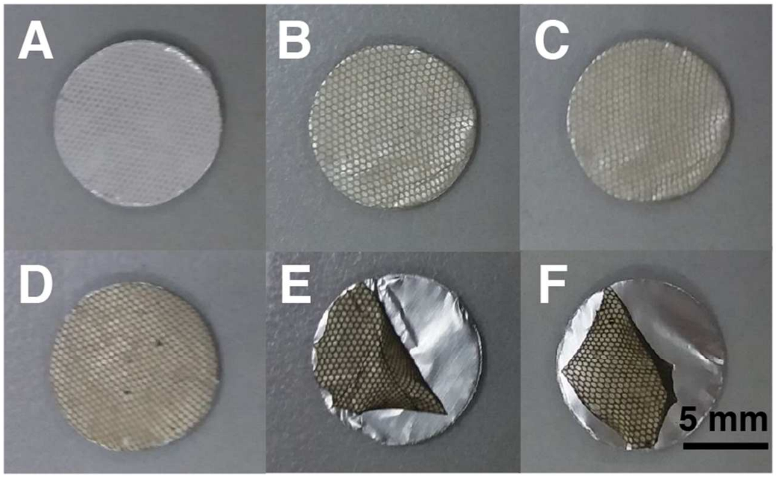

Figure S6. Photographs of (A) 0CS-, (B) 10CS-, (C) 20CS-, (D) 30CS-, (E) 40CS- and (F) 50CS-PLA/PCL membranes physically fixed on aluminum foils after exposure to 808-nm laser irradiation under dry condition at the power density of 0.50 W▪cm^{-2} for 5 min. 0CS-, 10CS-, 20CS- and 30CS-PLA/PCL membranes showed no obvious change in shape under irradiation as compared to the seriously damaged morphologies of 40CS- and 50CS-PLA/PCL membranes.

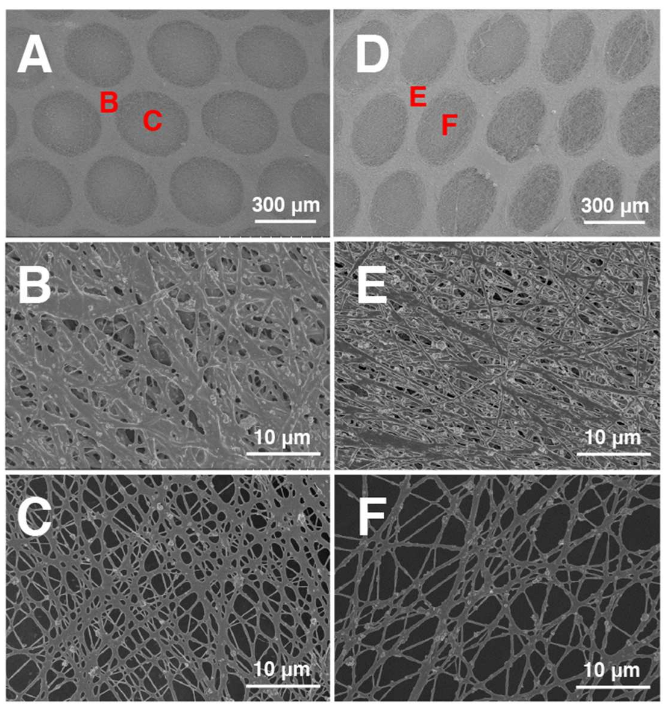

Figure S7. Representative SEM images of (A-C) 30CS- and (D-F) 40CS-PLA/PCL membranes under dry condition after exposure to 808-nm laser irradiation at the power density of 0.50 W▪cm^{-2} for 5 min. (B, E) and (C, F) shows the dense and loose fibrous structure in different membrane regions indicated in (A, D) at high magnification, respectively. 30CS-PLA/PCL membranes preserved better macroporous pattered structures than 40CS-PLA/PCL membranes after irradiation.

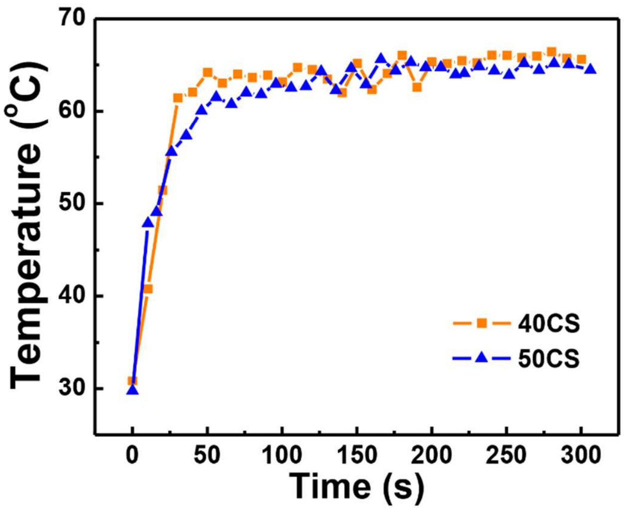

Figure S8. Photothermal heating curves of 40CS- and 50CS-PLA/PCL membranes in the dry environments under continuous irradiation of the 808-nm laser at 0.50 W▪cm^{-2} for 5 min.

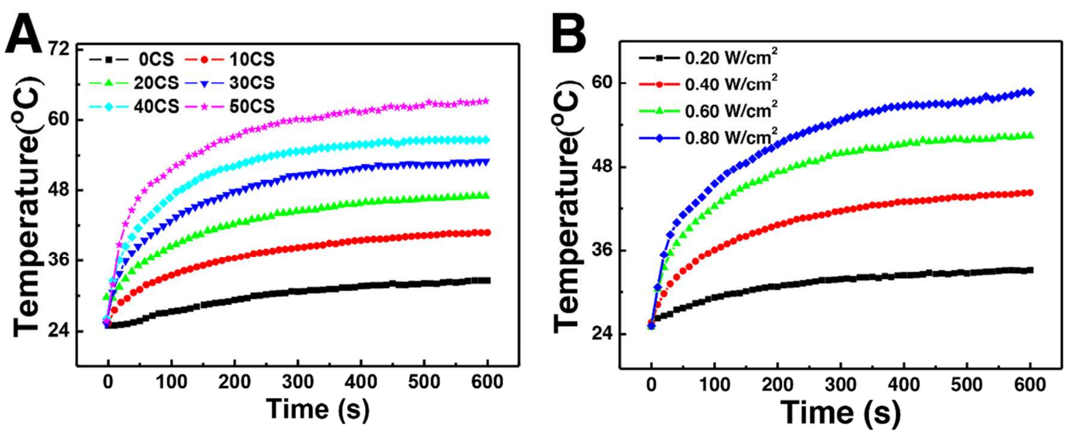

Figure S9. Photothermal heating curves of CS-PLA/PCL membranes immersed in 500 mL phosphatic buffer solution (PBS) under 808-nm laser irradiation with (A) different Cu2S contents at power density of 0.50 W▪cm^{-2} and (B) 30CS-PLA/PCL with various power densities indicated for 10 min. The photothermal temperature could be efficiently controlled between room temperature and 62 °C by altering laser power densities and Cu_2S contents.

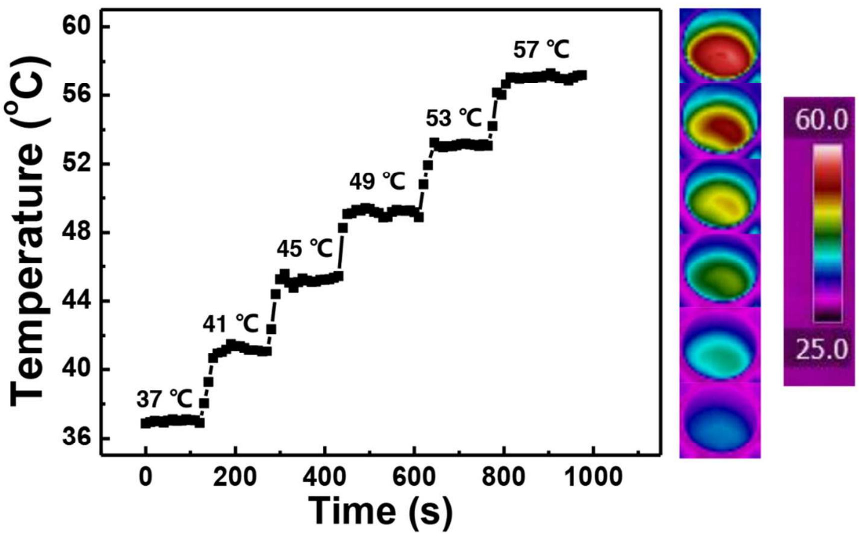

Figure S10. Heating curves and the corresponding near infrared images of 30CS-PLA/PCL membranes with controllable temperature under the wet condition.

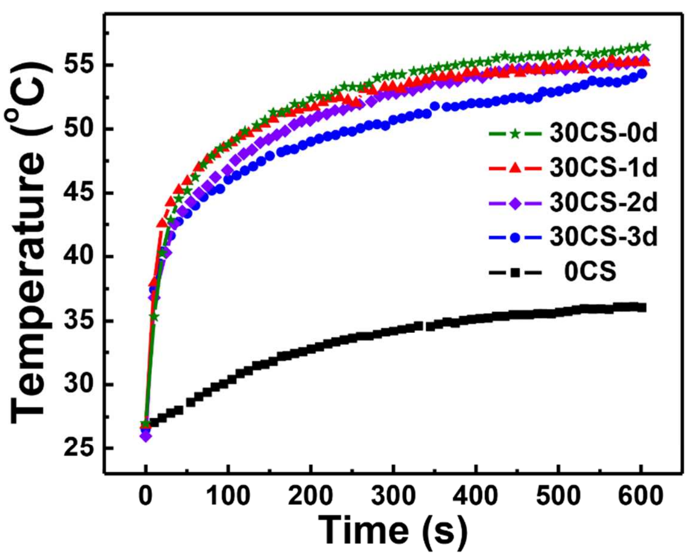

Figure S11. Photothermal heating curves of 30CS-PLA/PCL membranes after being soaked in cell medium for 0, 1, 2, 3 days (0.60 W•cm^{-2}, 10 min, 37 °C). Cu_2S-incorporated membranes could remain their excellent photothermal performance with slightly decrease in temperature elevation.

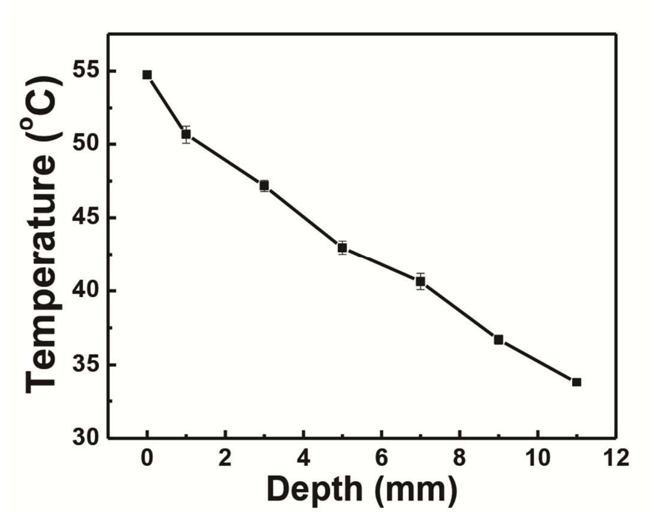

Figure S12. Final temperature of the pork at various depths (0, 1, 3, 5, 7, 9 and 11 mm), top of which was coved by 30CS-PLA/PCL membranes and then irradiated by the 808-nm laser at the power density of 0.40 W•cm^{-2} for 10 min at room temperature.

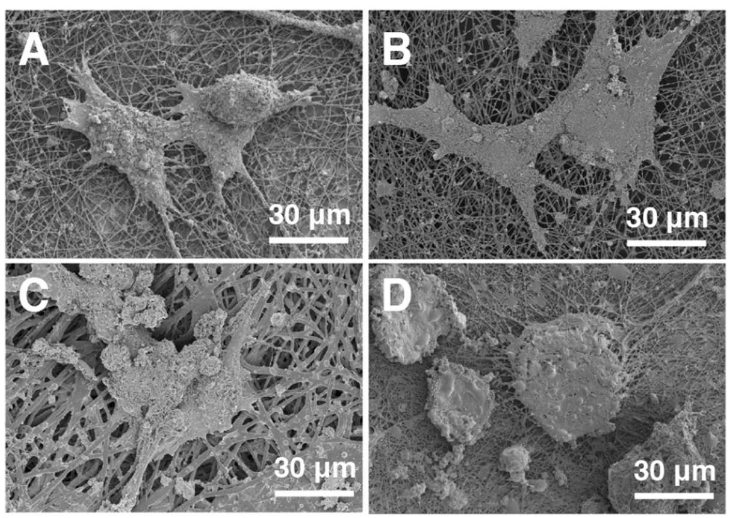

Figure S13. Morphologies of skin tumor cells after photothermal therapy. SEM images of skin tumor cells (murine B16F10 melanoma cells) on membranes treated with (A) 0CS- or (B) 30CS-PLA/PCL membranes without laser irradiation and (C) 0CS- or (D) 30CS-PLA/PCL membranes with laser irradiation (808 nm, 0.50 W•cm^{-2}, 15 min). The cellular morphologies in the three control groups kept unchanged with affluent pseudopods, while the tumor-cell morphology was seriously damaged in the laser-irradiated 30CS-PLA/PCL membranes.

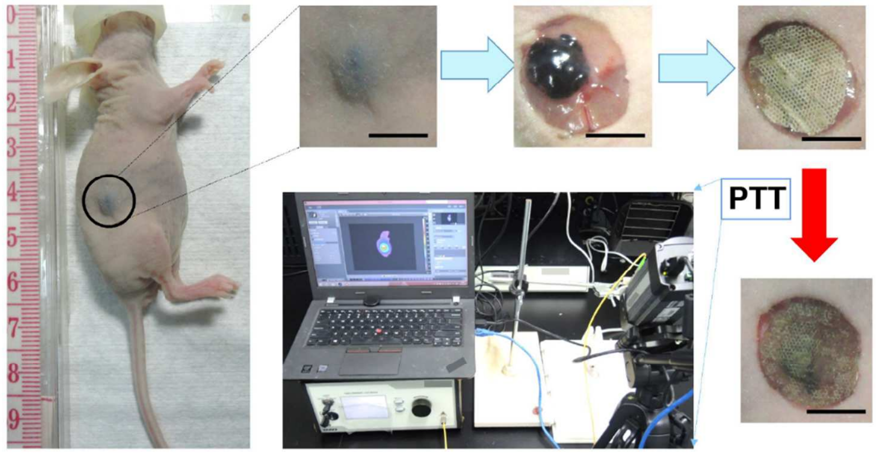

Figure S14. Experimental procedure of *in vivo* photothermal therapy. A full thickness wound (diameter = 10 mm) was created in the tumor site of tumor-bearing mice. 30CS-PLA/PCL membranes were used to cover the wound area, which was then exposed to the 808-nm laser irradiation at a power density of 0.40 W▪cm^{-2} for 15 min. Scale bar, 5 mm.

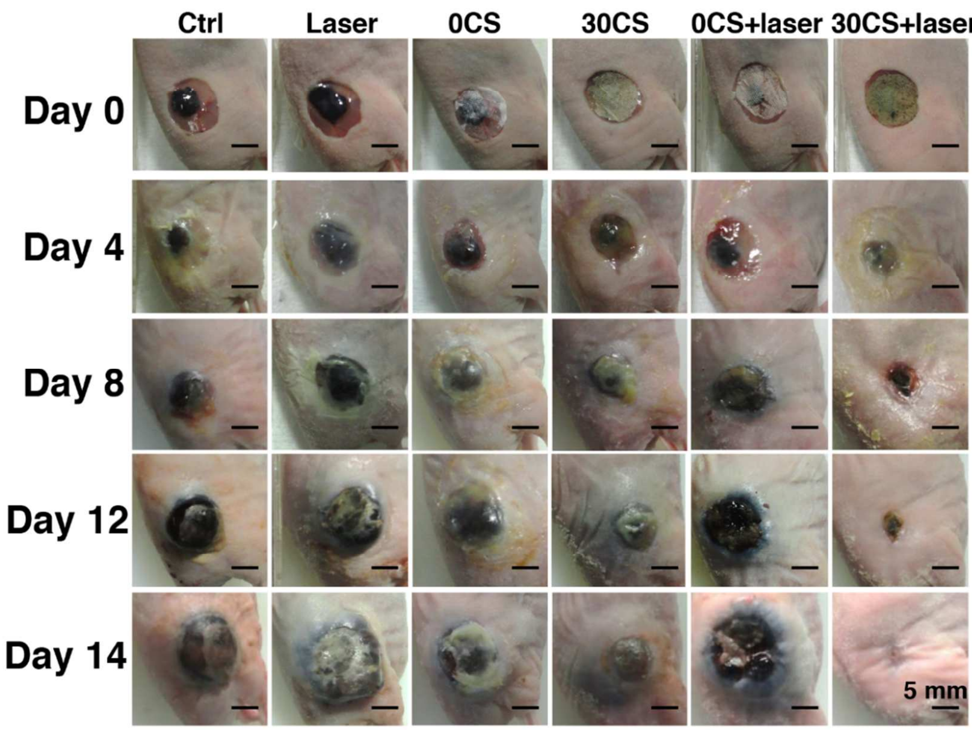

Figure S15. Representative skin wound photographs of tumor-bearing mice treated after various different treatments indicated taken on day 0, 4, 8, 12 and 14. Scale bar: 5 mm. The tumor volume of the 30CS-PLA/PCL+laser group was reduced after 4 days of irradiation, gradually disappeared with black scars left at the original sites after 8 days and the wound even completely healed without tumor recurrence within 14 days.

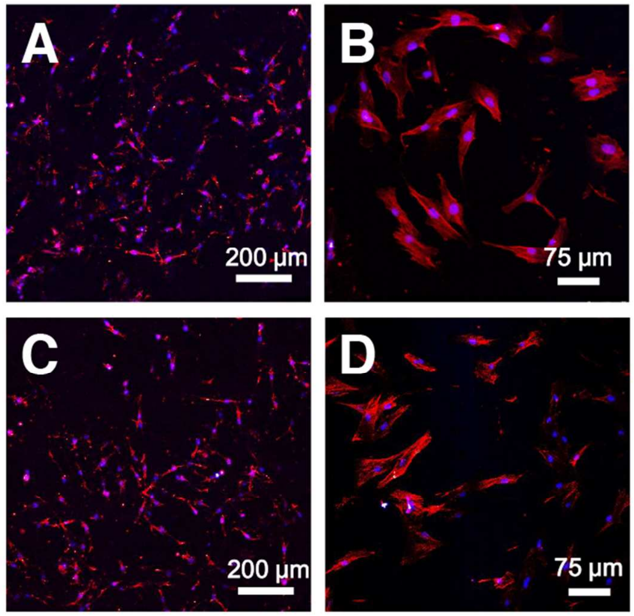

Figure S16. Morphologies of skin cells attached to CS-PLA/PCL membranes. Confocal LSM (red: cytoskeleton; blue: cell nuclei) images of human dermal fibroblasts (HDFs) after seeding on the (A, B) 0CS-PLA/PCL or (C, D) 30CS-PLA/PCL membranes for 24 h. Both 0CS- and 30CS-PLA/PCL membranes supported the adhesion and spreading of skin cells.

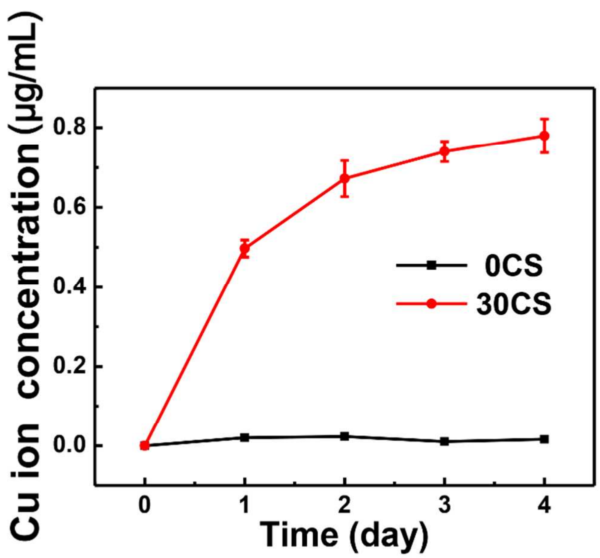

Figure S17. Cumulative amount of Cu ions released from 0CS-and 30CS-PLA/PCL membranes into Dulbecco's modified Eagle's medium (DMEM) as a function of immersion time at 37 °C.

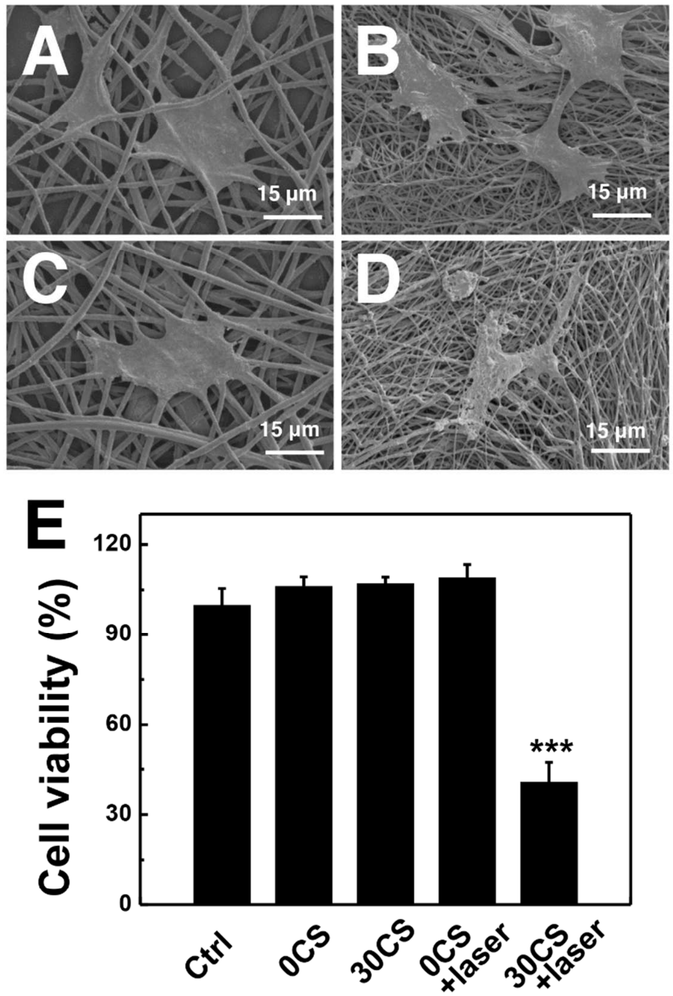

Figure S18. The photothermal effect on normal skin cells. Representative SEM images of human umbilical vein endothelial cells (HUVECs) on membranes treated with (A) 0CS- or (B) 30CS-PLA/PCL membranes without laser irradiation and (C) 0CS- or (D) 30CS-PLA/PCL membranes with laser irradiation (808 nm, 0.50 W▪cm^{-2}, 15 min). (E) Relative cell viability of HUVECs treated with 0CS- or 30CS-PLA/PCL membranes without NIR treatment and 0CS- or 30CS-PLA/PCL membranes with NIR treatment (808 nm, 0.50 W▪cm^{-2}, 15 min). The cellular morphologies were seriously damaged in the laser-irradiated 30CS-PLA/PCL membranes as compared to other three control groups, indicating normal skin cells could be killed by 30CS-PLA/PCL membranes under NIR irradiation.